http://dx.doi.org/10.5012/bkcs.2013.34.6.1625

Articles

Acetate-assisted Synthesis of Chromium(III) Terephthalate and Its Gas Adsorption Properties

Jing-jing Zhou,[†,‡] Kai-yu Liu,[†,*] Chun-long Kong,[‡,*] and Liang Chen[‡]

[†]*School of Chemistry and Chemical Engineering, Central South University, Changsha 410083, P.R. China*
[*]*E-mail: kaiyuliu@263.net*
[‡]*Ningbo Institute of Materials Technology and Engineering, Chinese Academy of Sciences, Ningbo 315201, P.R. China*
[*]*E-mail: kongchl@nimte.ac.cn*
Received February 7, 2013, Accepted March 2, 2013

We report a facile synthetic approach of high-quality chromium(III) terephthalate [MIL-101(Cr)] by acetate-assisted method in the absence of toxic HF. Results indicate that the morphology and surface area of the MIL-101(Cr) can be tuned by modifying the molar ratio of acetate/$Cr(NO_3)_3$. The Brunauer-Emmett-Teller (BET) surface area of MIL-101(Cr) synthesized at the optimized condition can exceed 3300 m^2/g. It is confirmed that acetate could promote the dissolution of di-carboxylic linker and accelerate the nucleation ratio. So the pure and small size of MIL-101(Cr) with clean pores can be obtained. CO_2, CH_4 and N_2 adsorption isotherms of the samples are studied at 298 K and 313 K. Compared with the traditional method, MIL-101(Cr) synthesized by acetate-assisted method possess enhanced CO_2 selective adsorption capacity. At 1.0 bar 298 K, it exhibits 47% enhanced CO_2 adsorption capacity. This may be attributed to the high surface area together with clean pores of MIL-101(Cr).

Key Words : MIL-101(Cr), Acetate-assisted synthesis, Gas adsorption, CO_2

Introduction

Metal-organic frameworks (MOFs), a new class of porous materials which are built from organic linkers and inorganic metal (or metal-containing cluster) nodes, possess high structural and chemical tunability.[1] They have been reported with a wide variety of pore sizes, volumes, and functionalities, which promote their potential applications in many fields such as gas storage and separation,[2-4] molecular recognition[5] and catalysis.[6] In recent years, significant efforts have been made in developing new MOFs and expanding their potential applications.[7-9] However, improvements in the reproducible synthesis approach of high surface area MOFs are still required for industrial application.

Indeed, many parameters such as compositional (*e.g.*, reaction stoichiometry, pH, solvent) and process parameters are extremely important for the formation of high-quality MOFs.[10] In this respect, some new methods have been developed for MOFs synthesis such as microwave-assisted route,[11,12] ultrasound-assisted approach,[13] mechanochemical method,[14,15] electrochemical synthesis,[16] DGC (dry gel conversion) method[17] and template assisted synthesis.[18] In addition, mineralizers such as fluorides,[19,20] TEOS and H_2O_2[21,22] even graphene oxide[23] also play key roles in the direction of structure and morphology for MOFs. Although many efforts have been made in MOFs synthesis, assembly of reproducible and high-quality MOFs leaves much to be desired.

MIL-101(Cr) is originally synthesized by Férey *et al*.[20] Its excellent thermal and chemical stability, high mesoporosity and large surface area have been attracting a great deal of interests for practical applications.[24,25] Many studies have been focused on the synthesis of MIL-101(Cr) frameworks.[26-30] However, reproducible synthesis of high-quality MIL-101(Cr) routes still need to be developed. Although the BET surface area of MIL-101(Cr) can be up to 4200 m^2/g,[20] most of the reported surface areas by traditional method are in the range of 2500-3000 m^2/g.[28-31] In addition, developing environmental-friendly synthesis process is also critical necessary. Since certain harmful mineralizing agent such as HF and HCl are applied in the traditional synthesis route. To the best of our knowledge, very limited environmental-friendly routes for MIL-101 synthesis has been reported.

Jhung has demonstrated that relative high pH is beneficial for the formation of chromium trimmers and benzenedicarboxylate to obtain nano-sized MIL-101(Cr).[12] Inspired by the fact that the alkaline solution can promote the dissolution of H_2BDC. We postulate that appropriate addition of weak alkaline may be beneficial for the synthesis of high quality MIL-101(Cr) without the toxic mineralizing agent HF.

In this case, the weak alkaline acetate was employed to assist synthesis of MIL-101(Cr) in our work. Herein two kinds of acetate and their various concentrations in the precursors were investigated. The structure, morphology, surface area, thermal stability and gas adsorption properties of the as-pre-

pared samples were analyzed. Experimental results demonstrate that small MIL-101(Cr) crystals with high surface area are synthesized successfully. Furthermore, MIL-101(Cr) prepared by acetate-assisted approach exhibits enhanced CO_2 selective adsorption capacity when compared with that of the traditional method. We expect that this approach could also be applicable to the synthesis of high-quality carboxylate-based MOFs such as MIL-53, MIL-96 and other functionalized MOFs.

Experimental

Chemicals. 1,4-Benzene di-carboxylic acid (H_2BDC) was purchased from Sigma-Aldrich and hydrofluoric acid (HF) was purchased from Merck. Chromium nitrate [$Cr(NO_3)_3{\cdot}9H_2O$], *N,N*-dimethyl-formamide (DMF), ethanol (EtOH), potassium acetate (CH_3COOK) and lithium acetate (CH_3COOLi) were purchased from TCI. All chemicals were used as received from vendors without further purification. Distilled water was prepared in our laboratory.

Instruments and Measurements. Powder XRD patterns of all samples were obtained on a Bruker AXS D8 Advance diffractometer using CuKα radiation at room temperature. The scan range was from 3 to 30° at a step size of 0.02°. The crystal size and morphology were analyzed on a Field Emission SEM (Hitachi, S-4800). TG analyses were performed in N_2 (flow rate 200 mL·min^{-1}) from room temperature to 1073 K at a heating rate of 5 K min^{-1} using a Mettler Toledo apparatus. IR spectra were recorded from samples in KBr pellets on a TENSOR 27 apparatus. The BET surface area was calculated over the range of relative pressures between 0.05 and 0.20 with nitrogen adsorption isotherm at 77.3 K (ASAP 2020, Micromeritics). Adsorption isotherms of CO_2, CH_4 and N_2 were measured at 298 and 313 K by an apparatus from Setram France (PCTpro E&E). Before each measurement, the samples were evacuated at 160 ºC for 6 h. The adsorbed amounts were calculated by the volumetric method. All the gases used in the study have a minimum purity of 99.99%.

Synthesis of MIL-101(Cr). The acetate-assisted hydrothermal synthesis approach was conducted as follows. Firstly, 1,4-benzene di-carboxylic acid (H_2BDC) (664 mg, 4 mmol), $Cr(NO_3)_3{\cdot}9H_2O$ (1600 mg, 4 mmol) and a certain amount of acetate were dissolved in distilled water (25 mL, 1389 mmol). Here different molar ratios of $CH_3COOLi/Cr(NO_3)_3$ and $CH_3COOK/Cr(NO_3)_3$ were investigated. Secondly, the mixture was well-dispersed under ultrasonic condition for 30 min and then heated in a Teflon-lined autoclave at 200 ºC for 12 h under autogenous pressure. Next the yielded solid was doubly filtered by filter paper and sufficiently washed with distilled water and followed by centrifugation. Finally, the resulting precipitate was transferred to a Teflon-lined autoclave washed with hot ethanol at 90 ºC for 4 h for twice. The obtained product was dried under vacuum at 150 ºC overnight.

For comparison, the MIL-101(Cr) was prepared by the traditional method.[20] The purification is slightly different from the acetate-assisted method. First of all, DMF was used to dissolve the unreacted H_2BDC within the pore of the crude product. The following processes were the same to that described above. Reaction conditions and properties of the examined samples are summarized in Table 1.

Results and Discussion

Structural and Morphological Characterization. XRD diffraction method is employed to identify the phase of the as-synthesized product. In order to study the phase of samples synthesized by acetate-assisted method, powder XRD patterns of the as-synthesized samples by CH_3COOLi-assisted and traditional method are shown in Figure 1. Results show that the diffraction peak positions and relative diffraction intensities are consistent with the simulated XRD pattern of MIL-101(Cr) reported previously.[20] In addition, no diffraction peaks of recrystallized H_2BDC are found at $2\theta = 17.4°$, 25.2° or 27.9°, which indicates no existence of unreacted H_2BDC.

Table 1. Reaction conditions and results for the synthesis of MIL-101(Cr) by acetate-assisted method and traditional method

Sample No.	Reaction conditions			Reaction results			
	Method	Molar ratio[a]	pH (reactant mixture)	Phase	S_{BET}[b] (m^2/g)	$S_{Langmuir}$[b] (m^2/g)	Particle size[c] (nm)
A	Traditional	0:1	<1.00	MIL-101(Cr)	2971	4201	680(20)
B	CH_3COOLi-assisted	0.06:1	2.98	MIL-101(Cr)	3074	4324	350(10)
C	CH_3COOLi-assisted	0.15:1	3.25	MIL-101(Cr)	3401	4884	270(10)
D	CH_3COOLi-assisted	0.30:1	3.46	MIL-101(Cr)	3252	4650	180(10)
E	CH_3COOLi-assisted	0.45:1	3.66	MIL-101(Cr)	3031	4332	120(10)
F	CH_3COOLi-assisted	1.00:1	3.85	MIL-101(Cr)	2217	3349	80(10)
G	CH_3COOLi-assisted	2.00:1	4.03	Unknown	1484	2097	ND[d]
H	CH_3COOK-assisted	0.06:1	2.99	MIL-101(Cr)	3093	4379	330(10)
I	CH_3COOK-assisted	0.15:1	3.26	MIL-101(Cr)	3398	4900	240(10)
J	CH_3COOK-assisted	0.30:1	3.50	MIL-101(Cr)	3267	4683	150(10)
K	CH_3COOK-assisted	2.00:1	4.00	Unknown	1567	2230	ND

[a]Molar ratio of acetate to $Cr(NO_3)_3$. [b]The specific surface area was calculated in the P/P_0 range of 0.05-0.2. [c]The average particle sizes were estimated from the SEM images and the deviations were given in brackets. [d]ND: not determined.

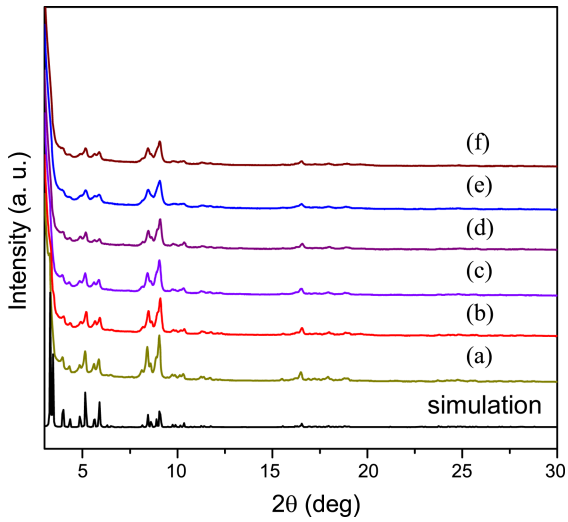

Figure 1. Powder XRD patterns for MIL-101(Cr) samples prepared by acetate-assisted approach and traditional method: (a)-(f) correspond to sample A to F. Simulated XRD pattern for MIL-101(Cr) is also present.

Thus, well-defined MIL-101(Cr) frameworks are successfully prepared by the acetate-assisted approach.

It should be noted that samples synthesized by acetate-assisted method show broader and weaker Bragg reflections of the XRD patterns than that of traditional method. The trend becomes more obvious when the molar ratio of acetate/$Cr(NO_3)_3$ increases from 0.06 to 1.00. It thus implies that the particle size of MIL-101(Cr) becomes smaller with increasing the acetate contents.[27] The change is also can be confirmed by the SEM images of samples in Figure 2. We believe that the change is mainly ascribed to the fact that acetate could enhance the solubility of organic linker and promote the deprotonation of di-carboxylic linkers in the water. Then the formation of chromium trimers are assuredly accelerated due to the high concentration of available di-carboxylate.[32] As a result, smaller crystal can be obtained due to the higher ratio of nucleation than growth aroused by the increased concentration of di-carboxylate and chromium trimmers. Similar mechanism has been elaborated in the synthesis of nano-sized MIL-101(Cr) by Jhung.[12]

To prove the truth, the pH values of the reactant mixtures are measured before the reaction (Table 1). The pH values of three other solutions are list in Table S1 for compare. It is obvious that the pH value of solution consisted of H_2BDC/$Cr(NO_3)_3$/H_2O without acetate addition is the lowest as 2.44.

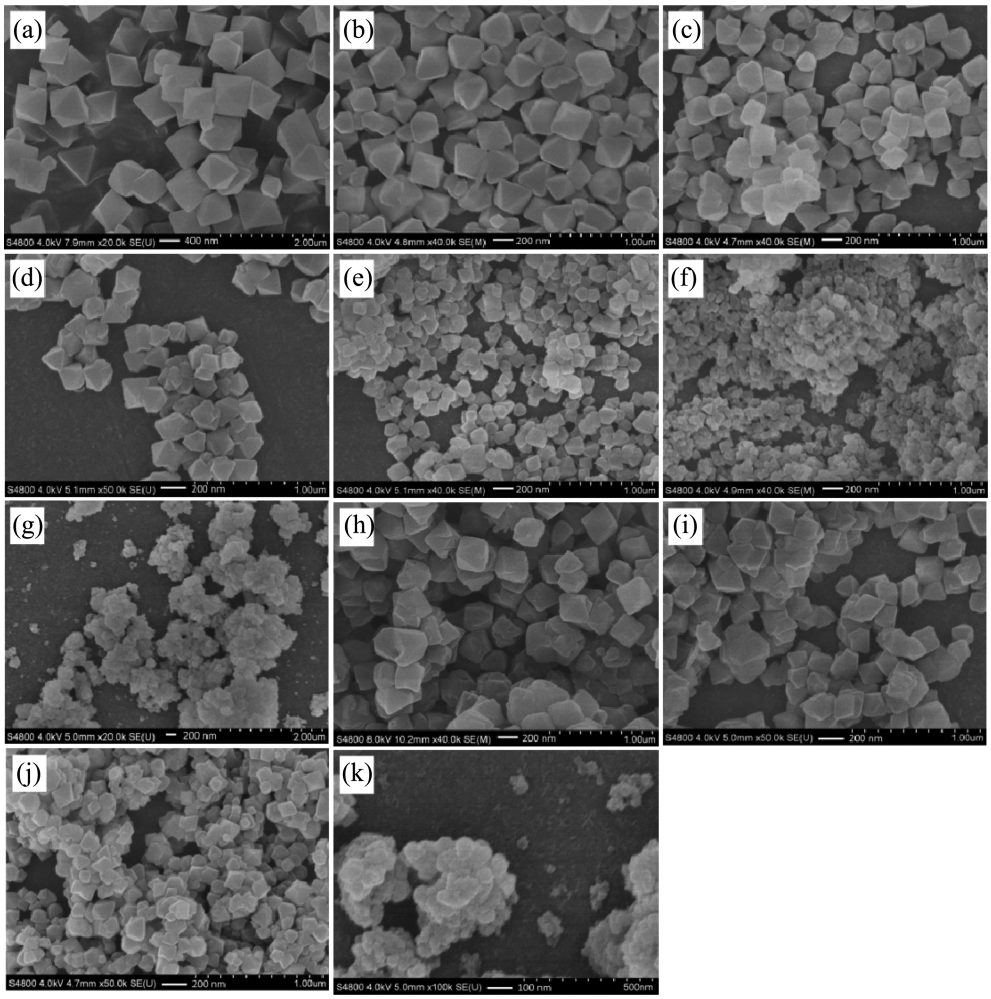

Figure 2. SEM images of MIL-101(Cr) samples synthesized by traditional method and acetate-assisted method: (a)-(k) correspond to sample A to K.

Here we take CH_3COOLi as example to illustrate the role of acetate in the dissolution of H_2BDC. When the molar ratio of $CH_3COOLi/Cr(NO_3)_3$ is same as 0.15:1. The pH value of the solution consisted of $CH_3COOLi/Cr(NO_3)_3/H_2O$ is 3.33, while the pH value is 3.25 for $CH_3COOLi/Cr(NO_3)_3/H_2BDC/H_2O$. Since H_2BDC is not soluble in the water, the difference of pH values between the two solutions is only caused by the dissolution of H_2BDC which promoted by CH_3COOLi. The same conclusion can also be drawn when the molar ratio is 1.00:1. Therefore, the acetate indeed promotes the dissolution of H_2BDC in the water.

As shown in Figure 2, MIL-101(Cr) crystals prepared by the traditional method have a cubo-octahedral shape and uniform size around 680 nm in diameter. In contrast, the size of samples prepared by the acetate-assisted approach decreases from 350 nm to less than 100 nm with the molar ratio of acetate/$Cr(NO_3)_3$ increasing. However, the products become amorphous and agglomerate seriously when the molar ratio exceeds 1.0. The particle sizes of MIL-101(Cr) prepared by traditional and acetate-assisted method are listed in Table 1.

Just as discussed above, the acetate could increase the solubility of H_2BDC, which accelerates the MOF nucleation rate and leads to the decrease of the crystal size.[32,33] When the acetate concentration is too low the deprotonation rate will be surely low and the particle size is not particularly small but still much smaller than that of traditional method. Then the influence becomes obvious with increasing the concentration of acetate. It should not be ignored that acetate may compete with the di-carboxylic linkers to coordinate with chromium ions in the reaction system,[18] which is unfavorable for the nucleation. Hence higher acetate concentration leads to smaller particles together with lower degree of crystallinity. The aggregation of MIL-101(Cr) crystals may be caused by the condensation of terminal functional group (such as carboxylic acid or hydroxyl group). When the molar ratio of acetate/$Cr(NO_3)_3$ increase higher than 1.00, the MIL-101(Cr) is hardly to be formed. Favorable pH values for the synthesis of high quality MIL-101(Cr) are 3.0-3.5 according to our research.

Surface Area Characterization. The BET surface areas of samples prepared with various molar ratios of acetate/$Cr(NO_3)_3$ are listed in Table 1. Which clearly shows that the concentration of acetate apparently determine the surface areas of as-prepared MIL-101(Cr). Interestingly, the surface areas first increase with increasing the ratios of acetate/$Cr(NO_3)_3$ and decrease with further increasing the ratios of acetate/$Cr(NO_3)_3$. The trend indicate that the optimal ratios of acetate/$Cr(NO_3)_3$ are located between 0.1 and 0.3.

Since the deprotonation of H_2BDC and the formation of chromium trimers are the two essential processes for the formation of MIL-101(Cr) structure according to the research.[32] Proper addition of acetate is beneficial for the dissolution of H_2BDC as well as the nucleation process, which are indispensable for the formation of small and intact MIL-101(Cr) particles. In addition, clean and unimpeded pores of MIL-101(Cr) can be obtained due to the increasing solubility of H_2BDC.[33] Reports have already demonstrated that the strategy of adding alkaline substances is efficient and facile for the yield of high quality MIL-101(Cr).[12,33]

Note that the sample synthesized by traditional method

Table 2. The summary of surface areas of the typically reported MIL-101(Cr)

Method	Acid	S_{BET} (m^2/g)	V_{pore} (cm^3/g)	Ref.
Traditional	HF	2578	1.25	[26]
Traditional	HF	2674	1.38	[31]
Traditional	HF	2693	1.30	[28]
Traditional	HF	2931	1.45	[29]
Traditional	no	2944	2.57	[30]
Traditional	HF	3200	2.10	[34]
Traditional	HF	4200	1.5-1.9	[20]
Microwave-assisted	HF	3360	1.75	[35]
Microwave-assisted	HF	3780	1.74	[24]
Traditional	no	2971	1.62	This work
CH_3COOLi-assisted	no	3401	1.83	
CH_3COOK-assisted	no	3398	1.79	

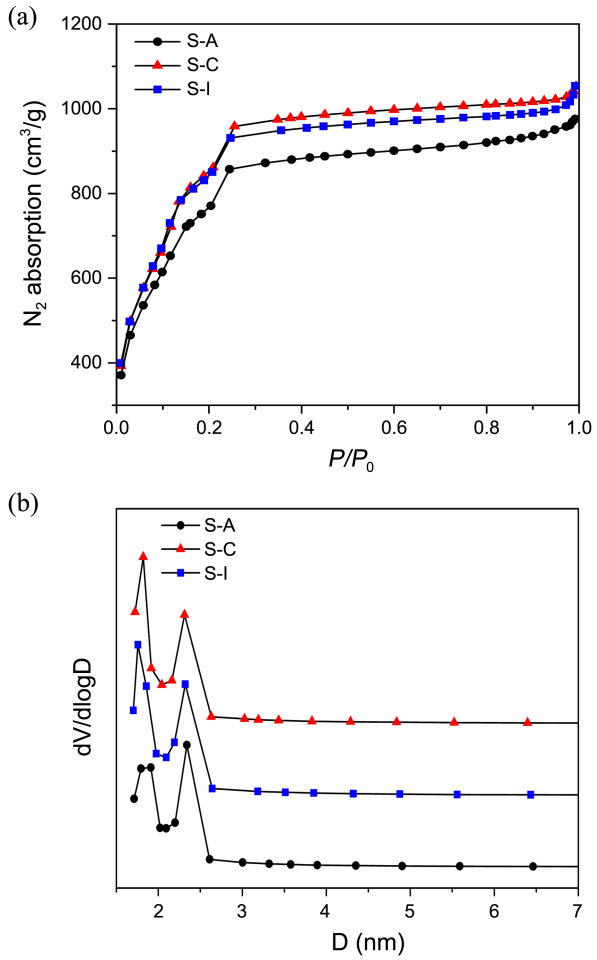

Figure 3. Nitrogen adsorption isotherms (a) and pore size distribution curves (b) of MIL-101(Cr) synthesized by traditional method and acetate-assisted method at 77.3 K: sample S-A, S-C and S-I.

displays low BET surface areas as 2971 m^2/g. We further summarize the properties of typically reported MIL-101(Cr) in Table 2. It can be seen that the BET surface area of MIL-101(Cr) prepared by traditional method in our work is comparable to the report. Obviously, the BET surface areas of samples prepared by acetate-assisted approach are higher than most MIL-101(Cr) prepared by traditional method reported in literatures. That is possibly owing to the small particles of MIL-101(Cr) with clean pores.

Nitrogen adsorption isotherms and pore size distribution curves (calculate by BJH equation) of three typical samples: Sample A, Sample C and Sample I (denoted as S-A, S-C and S-I) that synthesized by traditional method and acetate-assisted method are shown in Figure 3. The three samples exhibit similar Type I isotherms to the report.[12,20] Two uptake steps near $P/P_0 = 0.1$ and $P/P_0 = 0.2$ reflect the presence of two kinds of microporous windows in the structure. It is worth noting that the pore volume calculated at $P/P_0 = 0.99$ are 1.62 1.83, and 1.79 cm^3/g for S-A, S-C and S-I respectively. Which indicates that acetate could promote the dissolution of H_2BDC thus avoiding the block in the pores caused by the recrystallization of H_2BDC. The pore size distribution curves exhibit two different monodisperse pore sizes at about 1.8 and 2.3 nm, which is similar to the report.[27]

IR Spectra and Thermal Analysis. To identify the incorporation of H_2BDC into the resulting frameworks, the Infra-red spectra of three typical samples: Sample A, Sample C and Sample I (denoted as S-A, S-C and S-I) that prepared by traditional method and acetate-assisted method are presented in Figure S1. Clearly, vibrational bands characteristic of the framework -(O-C-O)- groups around 1510 and 1406 cm^{-1} confirm the presence of the di-carboxylate within MIL-101(Cr). Intense bands at around 3443 and 1625 cm^{-1} confirm the presence of a considerable number of water molecules within the framework. The IR spectra of the samples are consistent with that reported by Férey *et al.*[20] No band at around 1700 cm^{-1} that is characteristic of protonated carboxylic groups is observed in Figure S1, suggesting the absence of protonated carboxylic groups in the resulting frameworks.

To evaluate the stability of the as-prepared products, the thermal analysis (TGA) curves of the three samples are shown in Figure S2. Two main weight loss steps can be observed: the first loss (~10% of the initial weight) occurs at the temperature around 513 K, corresponding to the loss of guest molecules (*i.e.*, free water and ethanol molecules) in the framework. The second weight loss step (55-62% of the initial weight) occurs between 623 and 773 K, which is due to the elimination of -OH and other coordinated groups, leading to the decomposition of the frameworks. Results indicate that all samples show remarkable thermal stability with a decomposition temperature of 623 K in a nitrogen atmosphere.

Gas Adsorption Isotherms. To compare the adsorption properties of MIL-101(Cr) synthesized by traditional method and acetate-assisted method, gas adsorption isotherms are measured on Sample A, Sample C and Sample I (denoted as S-A, S-C and S-I). Here CO_2, CH_4 and N_2 adsorption isotherms of the three samples are measured at 298 and 313 K, respectively. Physical properties of the three gases are listed in Table S2.

Figure 4 shows the CO_2, CH_4 and N_2 adsorption properties of three samples at 298 K. CO_2 uptakes increase rapidly on S-A, S-C and S-I at low pressure and gradually become

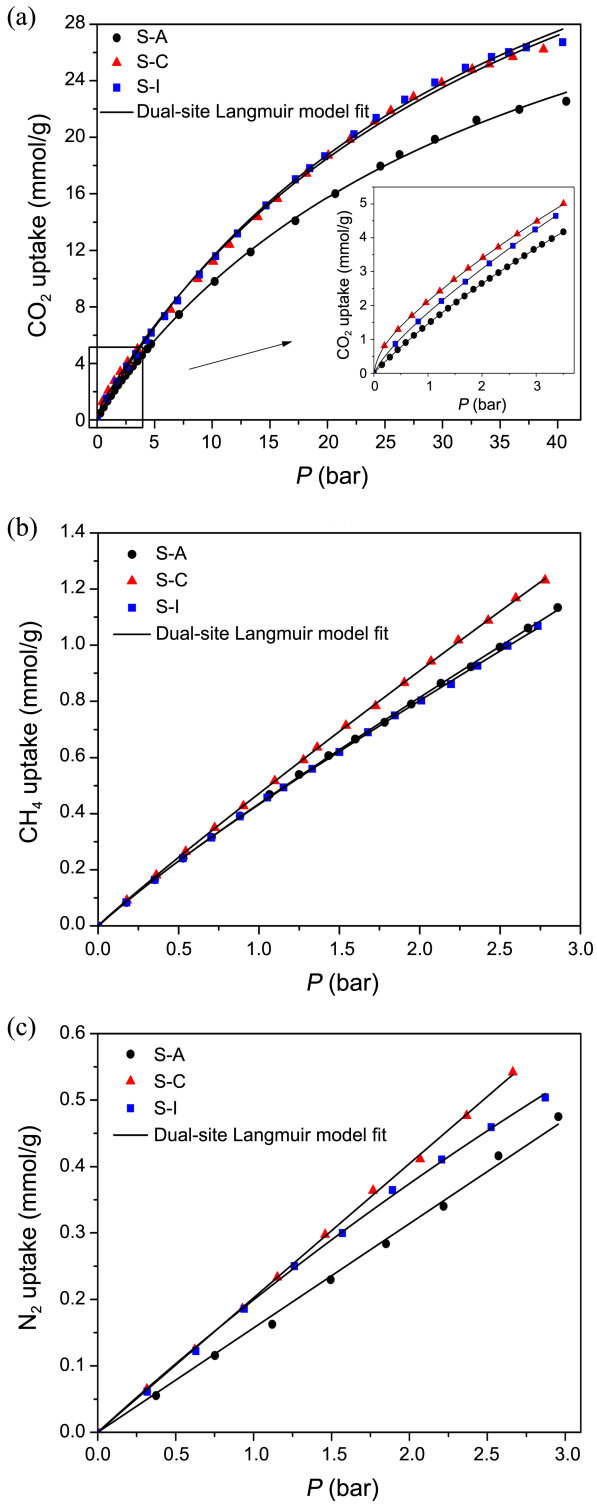

Figure 4. CO_2 (a), CH_4 (b) and N_2 (c) adsorption isotherms for sample S-A, S-C and S-I measured at 298 K and the fitted isotherms by Dual-site Langmuir (DSL) model respectively.

saturated at high pressure. Compared with CO_2, the uptakes of CH_4 and N_2 in the three samples are rather low and increase slightly with the increase of pressure. CH_4 uptakes of S-A, S-C and S-I are 0.44, 0.47 and 0.44 mmol/g at 1 bar and 0.15, 0.20 and 0.20 mmol/g for N_2 respectively. Which indicate that the interaction between CO_2 and frameworks is quite stronger than CH_4 and N_2.

Generally, the CO_2 adsorptive properties at lower-pressure (< 1.2 bar) and ambient temperatures (293-313 K) are predominantly dictated by the chemical features of the pore surface, while the surface area plays the dominant role at higher-pressure.[34] Here CO_2 has stronger interaction with MIL-101(Cr) than CH_4 and N_2 because it has higher polarizability and quadrupole moment (Table S2), which results in higher uptake of CO_2 than CH_4 and N_2. Although the size of CH_4 is slightly larger than N_2 CH_4 has a larger van der Waals potential parameter than N_2, therefore the interaction between CH_4 and framework is stronger than that of N_2. For this reason, the uptake of CH_4 is slightly higher than N_2 in MIL-101(Cr).

Figure 4(a) shows that S-C and S-I exhibit higher CO_2 uptakes than S-A at the entire pressure range. Moreover, the difference between S-A and S-C or S-A and S-I become distinct with increasing pressure. CO_2 uptake of S-A, S-C and S-I is up to 21.5, 25.4 and 25.9 mmol/g at 35 bar, respectively. As we know that the surface area determines the CO_2 uptakes at high pressure. Herein S-C (S_{BET} = 3401 m^2/g) and S-I (S_{BET} = 3398 m^2/g) distinctly show higher CO_2 uptakes than S-A (S_{BET} = 2971 m^2/g). Commonly, CO_2 capture is carried out at low pressure so that the CO_2 adsorption capacity at low pressure is critically important. Strikingly, the CO_2 uptakes at 1.0 bar 298 K are 2.13 and 1.77 mmol/g for S-C and S-I, which are 47% and 22% higher than S-A (1.45 mmol/g), respectively.

Therefore, MIL-101(Cr) prepared by acetate-assisted approach show enhanced CO_2 adsorption capacities. Gas adsorption isotherms of S-A, S-C and S-I at 313 K are also given in Figure S3-S5. The same conclusion can be drawn despite of the temperature increasing.

In reality, CO_2 is not the single component of the exhaust and flue gases, which usually contain other components such as N_2 and CH_4. Hence, an ideal CO_2 capture material should possess excellent selectivity for CO_2 in addition to the high adsorption capacity. In order to demonstrate the gas separation property, the adsorption equilibrium selectivity of CO_2 over N_2 and CO_2 over CH_4 at low pressure are evaluated according to Deng *et al.*[38] The Henry's law linear isotherm equation and the Dual Site Langmuir (DSL) model are used to fit the gases adsorption on MIL-101(Cr) as reported.[39-41]

The Henry's isotherm equation is

$$q = KP \tag{1}$$

Where q is the adsorbed amount per unit weight of adsorbent (mmol/g), P is the gas pressure at equilibrium (bar), K is the Henry's law constant [mmol/(g·bar)].

The Dual-site Langmuir (DSL) model is formulated as:

Table 3. The adsorption equilibrium selectivity calculated from the pure component adsorption isotherms

	S-A		S-C		S-I	
	298 K	313 K	298 K	313 K	298 K	313 K
CO_2/N_2	10.69	11.35	42.35	27.86	14.00	12.72
CO_2/CH_4	3.27	3.43	15.31	11.75	5.82	4.26

$$q = \frac{a_{m1}b_1P}{1+b_1P} + \frac{a_{m2}b_2P}{1+b_2P} \tag{2}$$

a_{mi} and b_i denotes saturation capacity and affinity parameters for sites of type i.

The Henry's constant K in this case is given by:

$$K = a_{m1}b_1 + a_{m2}b_2 \tag{3}$$

The adsorption equilibrium selectivity α_{AB} between components A and B is defined as

$$\alpha_{AB} = \frac{X_A}{X_B} \times \frac{Y_B}{Y_A} \approx \frac{K_A}{K_B} \approx \frac{a_{m1}b_1 + a_{m2}b_2}{a_{m1'}b_{1'} + a_{m2'}b_{2'}} \tag{4}$$

X_A and X_B are the molar fractions of components A and B on the adsorbent surface (or in the adsorbed phase), Y_A and Y_B are the molar fractions of components A and B in the gas phase. K_A and K_B are the Henry's constants for components A and B.

Results show that the model fits the isotherms very well ($R^2 > 0.999$), the fit parameters are listed in Table S3 and S4. The low pressure adsorption isotherms of CO_2, CH_4 and N_2 for S-A, S-C and S-I at 298 K and 313 K as well as the fitted isotherms by Dual-site Langmuir (DSL) model are showed in Figure 4 and Figures S3-S5, respectively.

Herein we calculated the adsorption equilibrium selectivity α_{AB} (Table 3) based on the fitted parameters. Apparently, S-C and S-I display better selectivity both of CO_2 over N_2 and CO_2 over CH_4 than S-A, which is favorable for selective adsorption CO_2 from their mixtures. The enhanced selectivity for S-C and S-I is probably caused by the increase of polarizability in the frameworks because some CH_3COO^- ions may coordinated with the terminal sites.[36] Besides, the higher specific surface area and pore volume are also quite important factors that can not be ignored. Further research is to be conducted to confirm the fact.

Conclusion

In this study, we demonstrate a facile synthesis of high-quality MIL-101(Cr) by acetate-assisted approach. It is confirmed that acetate could promote the dissolution of dicarboxylic linker and accelerate the nucleation ratio of MIL-101(Cr). So the pure and small size of MIL-101(Cr) with clean pores can be obtained. XRD patterns and SEM images clearly indicate that pure MIL-101(Cr) crystals are successfully prepared. The as-prepared frameworks show high BET surface area (> 3300 $m^2 \cdot g^{-1}$). Gas adsorption characterization reveals that MIL-101(Cr) synthesized by acetate-assist ap-

proach possesses enhanced CO_2 adsorption ability over the entire tested pressure range. The CO_2 uptake of MIL-101(Cr) increases by 47% than that of traditional method at 1.0 bar 298 K. More importantly, MIL-101(Cr) exhibits better CO_2 selective adsorption property than that synthesized by traditional method. That is mainly attributed to the higher specific surface area and pore volume. Besides, CH_3COO^- may coordinate with the terminal site to some extent, which increases the polarizability and enhances the CO_2 adsorption capacity of the framework. Further research is to be conducted to confirm the fact. We anticipate that this approach is also favorable for synthesis of other carboxylate-based MOFs.

Acknowledgments. We gratefully acknowledge the financial support by the national science foundation of China (Grant No. 51072204, 51172249), natural science foundation of Ningbo (Grant No. 2012A610100), natural science foundation of Zhejiang province (Grant No. Y4100695). And the publication cost of this paper was supported by the Korean Chemical Society.

References

1. Li, J. R.; Sculley, J.; Zhou, H. C. *Chem. Rev.* **2012**, *112*, 869.
2. Ma, S. Q.; Sun, D. F.; Wang, X. S.; Zhou, H. C. *Angew. Chem. Int. Ed.* **2007**, *46*, 2458.
3. Rowsell, J. L. C.; Yaghi, O. M. *Angew. Chem. Int. Ed.* **2005**, *44*, 4670.
4. Rowsell, J. L. C.; Spencer, E. C.; Eckert, J.; Howard, J. A. K.; Yaghi, O. M. *Science* **2005**, *309*, 1350.
5. Chen, B. L.; Yang, Y.; Zapata, F.; Lin, G. N.; Qian, G. D.; Lobkovsky, E. B. *Adv. Mater.* **2007**, *19*, 1693.
6. Huang, Y.; Zheng, Z.; Liu, T.; Lü, J.; Lin, Z.; Li, H.; Cao, R. *Catal. Commun.* **2011**, *14*, 27.
7. Horcajada, P.; Surble, S.; Serre, C.; Hong, D. Y.; Seo, Y. K.; Chang, J. S.; Greneche, J. M.; Margiolaki, I.; Férey, G. *Chem. Commun.* **2007**, *27*, 2820.
8. Bromberg, L.; Diao, Y.; Wu, H.; Speakman, S. A.; Hatton, T. A. *Chem. Mater.* **2012**, *24*, 1664.
9. Luo, J. H.; Xu, H. W.; Liu, Y.; Zhao, Y. S.; Daemen, L. L.; Brown, C.; Timofeeva, T.V.; Ma, S. Q.; Zhou, H. C. *J. Am. Chem. Soc.* **2008**, *130*, 9626.
10. Stock, N.; Biswas, S. *Chem. Rev.* **2012**, *112*, 933.
11. Jhung, S. H.; Lee, J. H.; Yoon, J. W.; Serre, C.; Férey, G.; Chang, J. S. *Adv. Mater.* **2007**, *19*, 121.
12. Khan, N. A.; Kang, I. J.; Seok, H. Y.; Jhung, S. H. *Chem. Eng. J.* **2011**, *166*, 1152.
13. Son, W. J.; Kim, J.; Kim, J.; Ahn, W. S. *Chem. Commun.* **2008**, *47*, 6336.
14. Friscic, T.; Reid, D. G.; Halasz, I.; Stein, R. S.; Dinnebier, R. E.; Duer, M. J. *Angew. Chem. Int. Ed.* **2010**, *49*, 712.
15. Klimakow, M.; Klobes, P.; Thunemann, A. F.; Rademann, K.; Emmerling, F. *Chem. Mater.* **2010**, *22*, 5216.
16. Hartmann, M.; Kunz, S.; Himsl, D.; Tangermann, O.; Ernst, S.; Wagener, A. *Langmuir* **2008**, *24*, 8634.
17. Ahmed, I.; Jeon, J.; Khan, N. A.; Jhung, S. H. *Cryst. Growth Des.* **2012**, *12*, 5878.
18. Pham, M. H.; Vuong, G. T.; Vu, A. T.; Do, T. O. *Langmuir* **2011**, *27*, 15261.
19. Barthelet, K.; Adil, K.; Millange, F.; Serre, C.; Riou, D.; Férey, G. *J. Mater. Chem.* **2003**, *13*, 2208.
20. Férey, G.; Mellot-Draznieks, C.; Serre, C.; Millange, F.; Dutour, J.; Surble, S.; Margiolaki, I. *Science* **2005**, *309*, 2040.
21. Huang, L. M.; Wang, H. T.; Chen, J. X.; Wang, Z. B.; Sun, J. Y.; Zhao, D. Y.; Yan, Y. S. *Micropor. Mesopor. Mater.* **2003**, *58*, 105.
22. Loiseau, T.; Lecroq, L.; Volkringer, C.; Marrot, J.; Férey, G.; Haouas, M.; Taulelle, F.; Bourrelly, S.; Llewellyn, P. L.; Latroche, M. *J. Am. Chem. Soc.* **2006**, *128*, 10223.
23. Liu, X.; Zhou, H.; Zhang, Y.; Liu, Y.; Yuan, A. *Chin. J. Chem.* **2012**, *30*, 2563.
24. Bernt, S.; Guillerm, V.; Serre, C.; Stock, N. *Chem. Commun.* **2011**, *47*, 2838.
25. Lebedev, O. I.; Millange, F.; Serre, C.; Van Tendeloo, G.; Férey, G. *Chem. Mater.* **2005**, *17*, 6525.
26. Li, Y. W.; Yang, R. T. *AIChE J.* **2008**, *54*, 269.
27. Jiang, D.; Burrows, A. D.; Edler, K. J. *CrystEngComm* **2011**, *13*, 6916.
28. Liu, Y. Y.; Ju-Lan, Z.; Jian, Z.; Xu, F.; Sun, L. X. *Int. J. Hydrogen Energy* **2007**, *32*, 4005.
29. Llewellyn, P. L.; Bourrelly, S.; Serre, C.; Vimont, A.; Daturi, M.; Hamon, L.; De Weireld, G.; Chang, J. S.; Hong, D. Y.; Hwang, Y. K.; Jhung, S. H.; Férey, G. *Langmuir* **2008**, *24*, 7245.
30. Senkovska, I.; Kaskel, S. *Micropor. Mesopor. Mater.* **2008**, *112*, 108.
31. Chowdhury, P.; Bikkina, C.; Gumma, S. *J. Phys. Chem. C* **2009**, *113*, 6616.
32. Khan, N. A.; Jun, J. W.; Jhung, S. H. *Eur. J. Inorg. Chem.* **2010**, *2010*, 1043.
33. Yang, J.; Zhao, Q.; Li, J.; Dong, J. *Micropor. Mesopor. Mater.* **2010**, *130*, 174.
34. Sumida, K.; Rogow, D. L.; Mason, J. A.; McDonald, T. M.; Bloch, E. D.; Herm, Z. R.; Bae, T. H.; Long, J. R. *Chem. Rev.* **2012**, *112*, 724.
35. Maksimchuk, N. V.; Timofeeva, M. N.; Melgunov, M. S.; Shmakov, A. N.; Chesalov, Y. A.; Dybtsev, D. N.; Fedin, V. P.; Kholdeeva, O. A. *J. Catal.* **2008**, *257*, 315.
36. Chen, Y. F.; Babarao, R.; Sandler, S. I.; Jiang, J. W. *Langmuir* **2010**, *26*, 8743.
37. Serre, C.; Millange, F.; Surble, S.; Férey, G. *Angew. Chem. Int. Ed.* **2004**, *43*, 6285.
38. Zhang, Z.; Huang, S.; Xian, S.; Xi, H.; Li, Z. *Energy Fuels* **2011**, *25*, 835.
39. Saha, D.; Bao, Z. B.; Jia, F.; Deng, S. G. *Environ. Sci. Technol.* **2010**, *44*, 1820.
40. Zheng, B.; Bai, J.; Duan, J.; Wojtas, L.; Zaworotko, M. J. *J. Am. Chem. Soc.* **2011**, *133*, 748.
41. Chowdhury, P.; Mekala, S.; Dreisbach, F.; Gumma, S. *Micropor. Mesopor. Mater.* **2012**, *152*, 246.